

# DOES ANYONE OUT THERE KNOW THE STRENGTH OF SAPPHIRE?

**Daniel C. Harris\***

Naval Air Systems Command, China Lake, California

**Abstract:** Results are compared for several different sets of 4-point flexure strength measurements on sapphire as a function of crystal orientation and temperature. The only consistent trend is that strength drops rapidly with increasing temperature when the c-axis of the crystal is the principal axis of tension and compression. Using Grafoil between sapphire and the load fixture increases the apparent strength of specimens whose principal axis is c by a factor of 2–3, but has little effect on other crystallographic orientations. The rate of crack propagation on the m-plane of sapphire increases by 7 orders of magnitude between 20 and 600°C.

## BACKGROUND

Sapphire is the most durable commercially available infrared window material. It has good optical properties in the 3-5  $\mu\text{m}$  wavelength atmospheric transmission window and it has the best resistance to erosion by rain and sand of any available window material. It also has excellent thermal shock resistance. However, its thermal shock resistance is limited by loss of mechanical strength above room temperature. Studies of the strength of sapphire with different crystal orientations, different finishes, and from different growth methods have shown that sapphire loses strength rapidly when heated above room temperature.<sup>1,2,3</sup> By contrast, the strength of polycrystalline alumina, which has the same chemical composition as sapphire ( $\text{Al}_2\text{O}_3$ ) is essentially constant up to 800°C and then begins to fall.<sup>2,4</sup>

The newest missiles with the most demanding flight profiles can generate thermal stresses in sapphire windows and domes that exceed the thermal shock resistance of the material. Active cooling can enable the window or dome to survive, but at the price of added weight, volume, and cost. If the strength of sapphire at elevated temperature were higher, the thermal shock resistance would be greater and cooling might not be necessary. The Office of Naval Research conducted an exploratory development program from 1996 to 2002 to try to enhance the high temperature strength of sapphire. Avenues that were explored included doping, annealing, polishing,<sup>5,6,7,8,9,10,11</sup> etching, ion implantation,<sup>12</sup> and neutron irradiation.<sup>13,14</sup>

The sapphire crystal in Figure 1 has 3-fold symmetry about the c-axis, which is also called the optical axis. Axes designated a and m are perpendicular to the c-axis. Three cleavage planes called rhombohedral planes (r planes) are symmetrically disposed about the c-axis.

---

\* Code 4T42A0D, 1 Administration Circle, Naval Air Systems Command, China Lake CA 93555;  
Phone 760-939-1649; harrisdc@navair.navy.mil.

Report Documentation Page				Form Approved OMB No. 0704-0188	
Public reporting burden for the collection of information is estimated to average 1 hour per response, including the time for reviewing instructions, searching existing data sources, gathering and maintaining the data needed, and completing and reviewing the collection of information. Send comments regarding this burden estimate or any other aspect of this collection of information, including suggestions for reducing this burden, to Washington Headquarters Services, Directorate for Information Operations and Reports, 1215 Jefferson Davis Highway, Suite 1204, Arlington VA 22202-4302. Respondents should be aware that notwithstanding any other provision of law, no person shall be subject to a penalty for failing to comply with a collection of information if it does not display a currently valid OMB control number.					
1. REPORT DATE <b>00 MAY 2002</b>		2. REPORT TYPE <b>N/A</b>		3. DATES COVERED <b>-</b>	
4. TITLE AND SUBTITLE <b>Does Anyone Out There Know The Strength Of Sapphire?</b>				5a. CONTRACT NUMBER	
				5b. GRANT NUMBER	
				5c. PROGRAM ELEMENT NUMBER	
6. AUTHOR(S)				5d. PROJECT NUMBER	
				5e. TASK NUMBER	
				5f. WORK UNIT NUMBER	
7. PERFORMING ORGANIZATION NAME(S) AND ADDRESS(ES) <b>Naval Air Systems Command, China Lake CA 93555</b>				8. PERFORMING ORGANIZATION REPORT NUMBER	
9. SPONSORING/MONITORING AGENCY NAME(S) AND ADDRESS(ES)				10. SPONSOR/MONITOR'S ACRONYM(S)	
				11. SPONSOR/MONITOR'S REPORT NUMBER(S)	
12. DISTRIBUTION/AVAILABILITY STATEMENT <b>Approved for public release, distribution unlimited</b>					
13. SUPPLEMENTARY NOTES <b>See also ADM201579., The original document contains color images.</b>					
14. ABSTRACT					
15. SUBJECT TERMS					
16. SECURITY CLASSIFICATION OF:			17. LIMITATION OF ABSTRACT <b>SAR</b>	18. NUMBER OF PAGES <b>15</b>	19a. NAME OF RESPONSIBLE PERSON
a. REPORT <b>unclassified</b>	b. ABSTRACT <b>unclassified</b>	c. THIS PAGE <b>unclassified</b>			

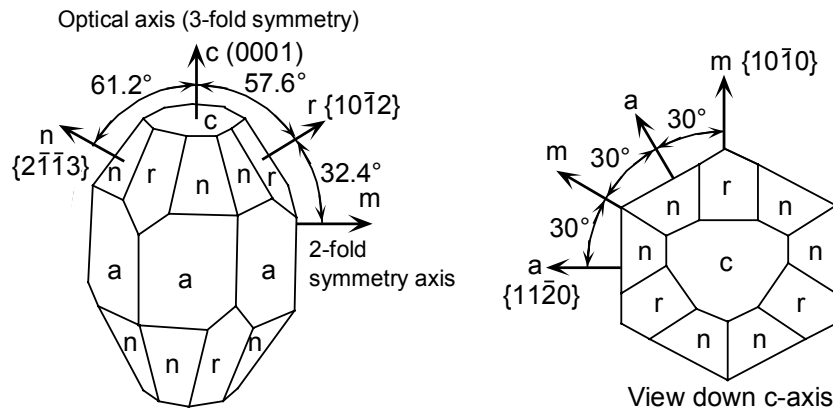


Figure 1. Sapphire crystal showing mineralogical and Miller index notation. The c-axis is a 3-fold symmetry axis, but sapphire is indexed as a hexagonal unit cell with  $c/a = 2.730$ .

In 1989, we measured the 4-point flexure strength of sapphire bars as a function of temperature in three crystal orientations (Type 1-3 in Figure 2). An additional orientation (Type 4 in Figure 2) was studied in the mid 1990s and a compendium of results was published in 1998<sup>15</sup>.

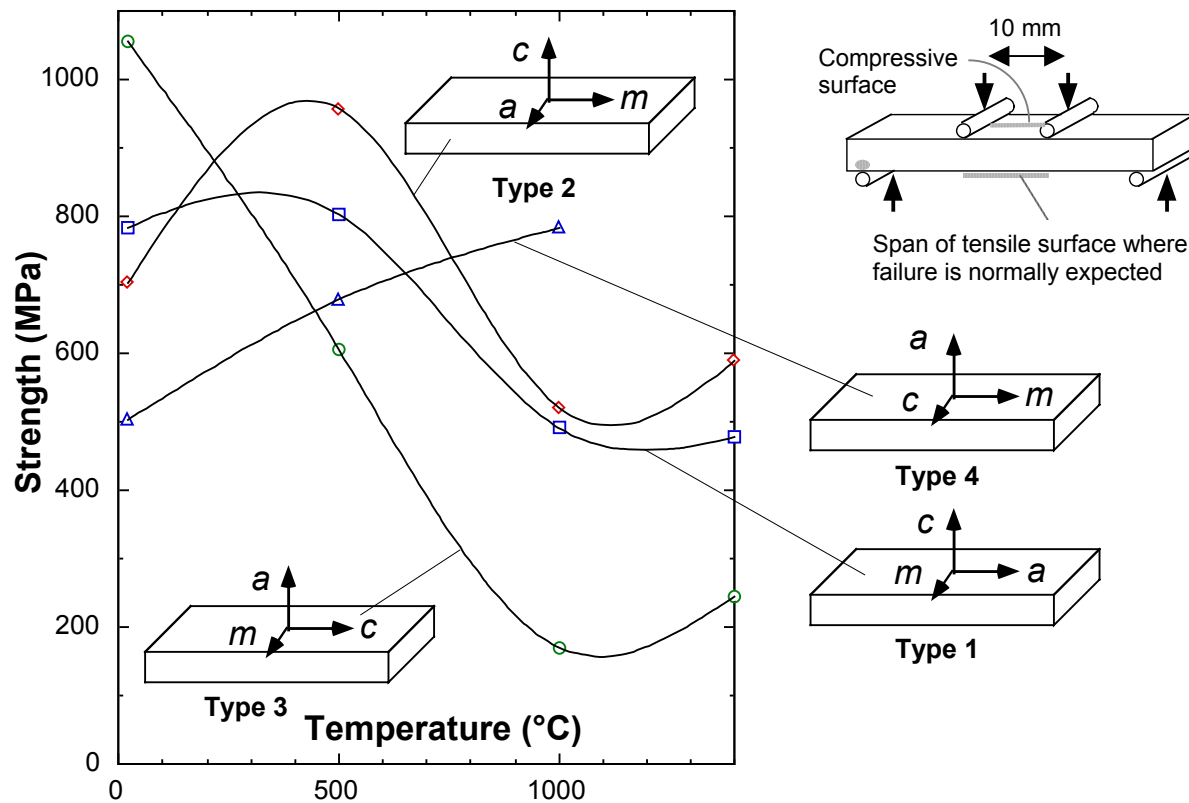


Figure 2. 4-Point flexure strength of sapphire as a function of crystal orientation and temperature as reported by Schmid and Harris in 1998.<sup>15</sup> Bars dimensions = 3 x 4 x 45 mm. Load span = 10 mm and support span = 40 mm. Each data point for Type 1-3 bars is the average of 34-40 results. Type 4 points are the average of only 5 results.

## HOW GENERAL ARE THE 4-POINT FLEXURE RESULTS?

In the late 1990s the joint Army-Navy-Air Force Sapphire Statistical Characterization and Risk Reduction (SSCARR) Program<sup>16,17</sup> measured 4-point flexure strength of 1500 sapphire bars meant to represent the material and finish of two missile windows (THAAD and Arrow) and one missile dome (Standard Missile 2 Block IVA). Additional 4-point flexure measurements were made by Crystal Systems, Inc. (CSI) for the Navy Exploratory Development program<sup>18</sup> and by the National Institute of Standards and Technology in a study of slow crack growth in sapphire.<sup>19</sup>

Figures 3 and 4 display all data for crystal orientations 1 and 2. Error bars are 90% confidence intervals for the mean. It is not surprising that specimens prepared at different times by different fabricators do not have the same strength. However, it is distressing to observe that different data sets do not have the same temperature dependence. Crystal Systems data from 1990 exhibit a small increase in strength between 20° and 500°C. THAAD window specimens generally decrease in strength between 20° and 300°C. THAAD specimens were all made from identical blanks of Crystal Systems sapphire, but fabricated by Vendors B and C. Strengths of bars from Vendor C are consistently ~50% greater than strengths from Vendor B. Figure 3 also shows CSI specimens from 2000 tested with 10 or 20-mm load spans. Type 1 specimens tested with the 20-mm load span are predicted to be ~25% weaker than those tested with the 10-mm load span because of the increased area under load (and assuming a Weibull modulus of ~3).

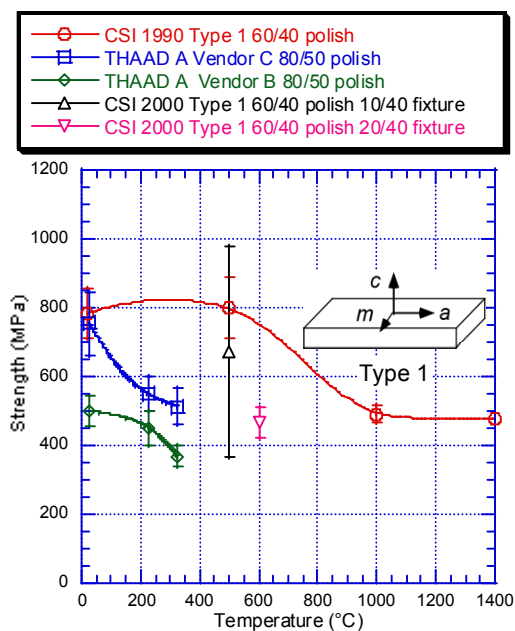


Figure 3. 4-Point flexure strengths of Type 1 sapphire bars. All bars are 3 x 4 x 45 mm and optically polished. All bars were tested with a 10 mm load span and 40 mm support span, except the last entry in the legend, which had a 20 mm load span.

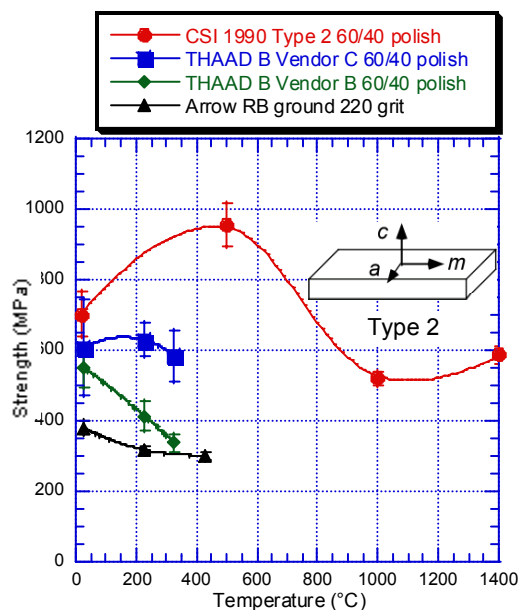


Figure 4. 4-Point flexure strengths of Type 2 sapphire bars. All bars were tested with a 10 mm load span and 40 mm support span. The Arrow RB bars had ground surfaces. All other bars were polished.

Sapphire is readily susceptible to failure in compression along the c-axis of the crystal at elevated temperature.<sup>15,20,21</sup> The c-axis is the axis of highest symmetry in the crystal. The a- and m-axes are each 2-fold symmetric, and are physically very similar to each other. It was proposed by Fred Schmid of Crystal Systems that the critical determinant of sapphire strength is the orientation of the c-axis with respect to the applied load. Following this idea, we expect that the mechanical properties of crystal orientations 1 and 2 ought to be very similar because in both cases the principal axis of tension or compression along the bar is a or m. The axis of the applied load is c. Grouping all the data for Type 1 and 2 bars in Figures 3 and 4 into one graph gives the results in Figure 5.

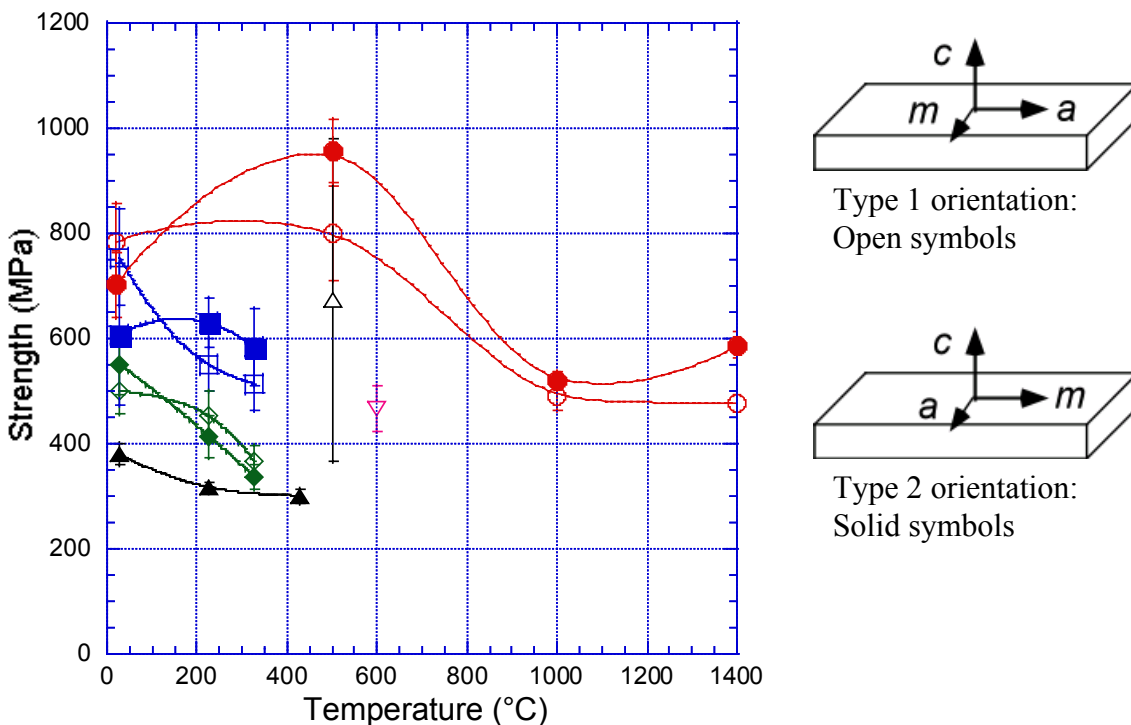


Figure 5. Composite graph showing 4-point flexure strength of Type 1 (open symbols) and Type 2 (solid symbols) sapphire bars from Figures 3 and 4.

We observe in Figure 5 that crystal orientations 1 and 2 do have similar behavior for corresponding sets of bars (filled and open circles, filled and open squares, and filled and open diamonds). The similar behavior confirms that the response to stress is very similar for the a and m axes, which are different from the c-axis.

Figures 6 and 7 show the behavior of crystal orientations 3 and 3a, in which the principal axis of tension and compression is c and the load is applied along the a or m direction. Figure 8 is a composite of Figures 6 and 7. The most noteworthy feature is the rapid decrease in strength with increasing temperature when c is the principal axis of tension and compression.

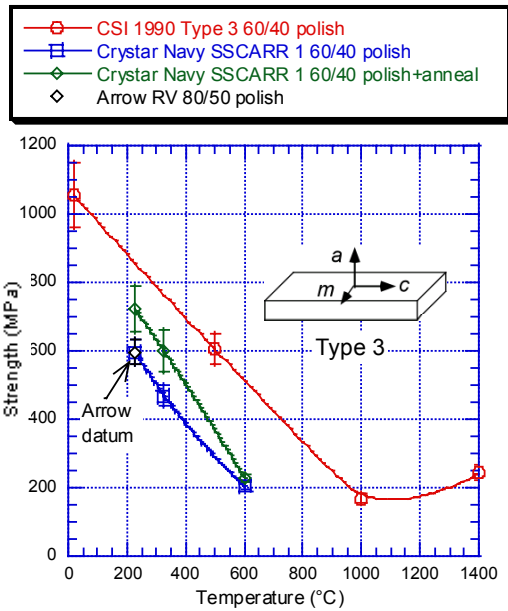


Figure 6. 4-Point flexure strengths of Type 3 sapphire bars. 3 x 4 x 45 mm polished bars were tested with a 10 mm load span and 40 mm support span. Annealing of one set of bars was at 1200°C for 24 h in air. Single datum for Arrow is superimposed on Crystar square point at 227°C.

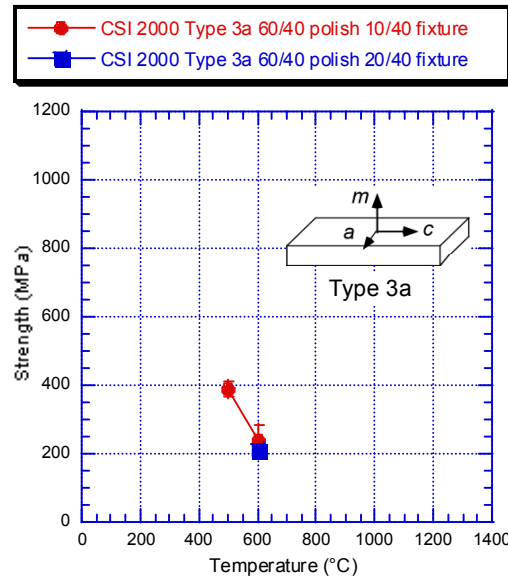


Figure 7. 4-Point flexure strengths of Type 3a sapphire bars tested with 40 mm support span and either 10 or 20 mm load span. The point for the 20-mm load span at 600°C is almost identical to the point for the 10-mm load span.

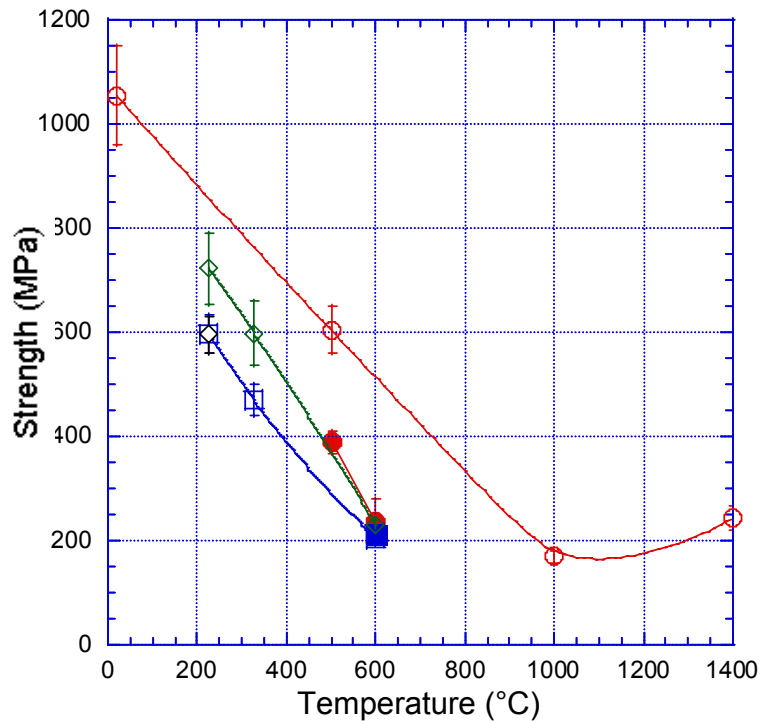


Figure 8. Composite graph showing 4-point flexure strength of Type 3 and Type 3a sapphire bars from Figures 6 and 7.

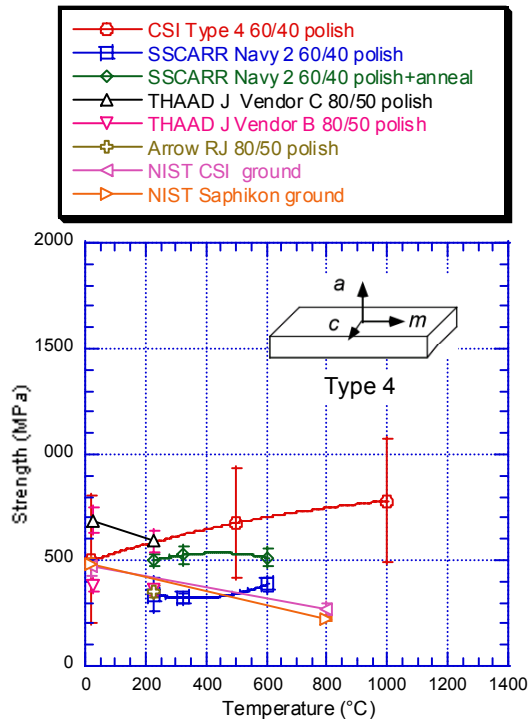


Figure 9. 4-Point flexure strengths of Type 4 sapphire bars.

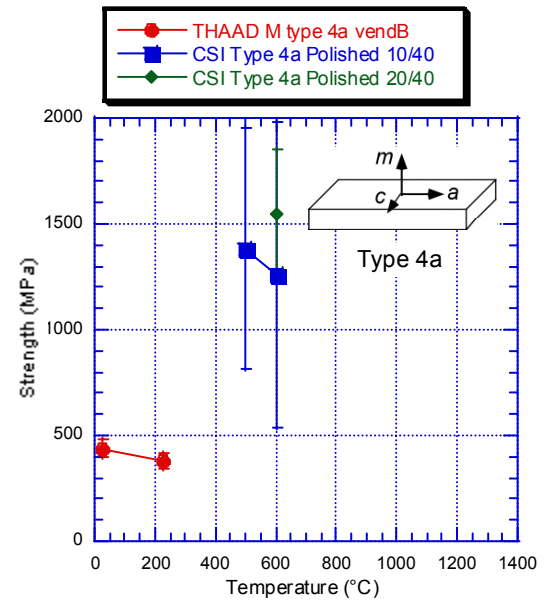
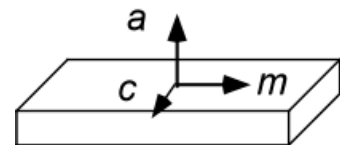
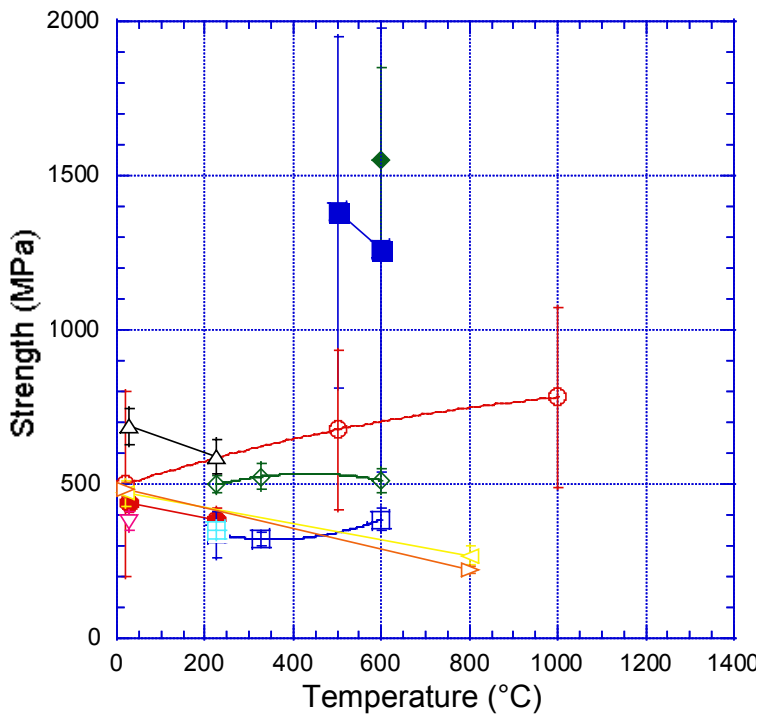
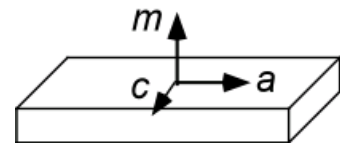


Figure 10. 4-Point flexure strengths of Type 4a sapphire bars.



Type 4 orientation:  
Open symbols



Type 4a orientation:  
Solid symbols

Figure 11. Composite graph showing 4-point flexure strength of Type 4 and Type 4a sapphire bars from Figures 9 and 10.

Figures 9-11 show the behavior of crystal orientations 4 and 4a, in which the principal axes of tension and compression and the direction of the applied load are all a or m. The c-axis is normal to the loads and should experience very little stress in type 4 and 4a bars. The earliest data set (open circles in Figure 9) suggested that the strength of type 4 bars increases between 20° and 1000°C. However, there were only 5 replications at each temperature and the standard deviations were large. The SSCARR Navy bars (open squares and open diamonds in Figures 9 and 11) represent many more replications and have a much smaller confidence interval for the mean. In these bars, the strength appears to be fairly constant over the temperature range 227° to 600°C. However, THAAD bars J and M lose strength between 20° and 227°C. Furthermore, two sets of measurements from the National Institute of Standards and Technology (NIST) on bars from Crystal Systems and from Saphikon are in close agreement with each other and show a loss of strength between 20° and 800°C. In Figure 10, different test sets have widely disparate strengths even though all bars were made from Crystal Systems material. In summary, there is little consistency between different sets of Type 4 and 4a specimens.

The question posed at the beginning of this section is whether there are consistent trends of strength with changes in temperature for the different crystal orientations. The only consistent trend seems to be that strength decreases rapidly with increasing temperature when the c-axis is the principal axis of tension and compression. There is no consistency in trends for the other crystal orientations when specimens from different sets of tests are compared.

## **EFFECT OF GRAFOIL ON FLEXURE STRENGTH MEASUREMENTS OF SAPPHIRE**

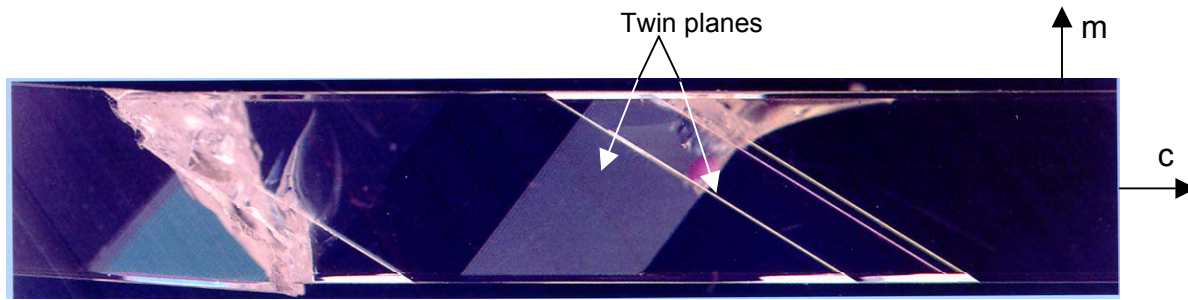
The compressive strength of sapphire decreases by 95% between 20° and 600°C when a c-axis sapphire cylinder is compressed between two rigid blocks of material, such as silicon carbide.<sup>15</sup> However, if a thin sheet of graphite (0.12-mm-thick Grafoil®) is placed between the sapphire and the load blocks, the strength at 600°C is about 4-5 times higher than the strength without Grafoil (~200-250 vs. ~50 MPa). It was shown that Grafoil reduces the extent of r-plane twin formation during c-axis compression at 600°C.<sup>18</sup> It was thought that Grafoil reduces the stress of point contacts between the microscopically rough surfaces of sapphire and silicon carbide and also that Grafoil reduces the friction that could prevent the flat end faces of the sapphire cylinder from spreading during compression.

Figure 12 shows the effect of placing Grafoil between the load rollers and the sapphire in a 4-point flexure test. When the c-axis was the principal axis of tension and compression, Grafoil reduced the incidence of twinning and increased the mean strength by more than a factor of 2.

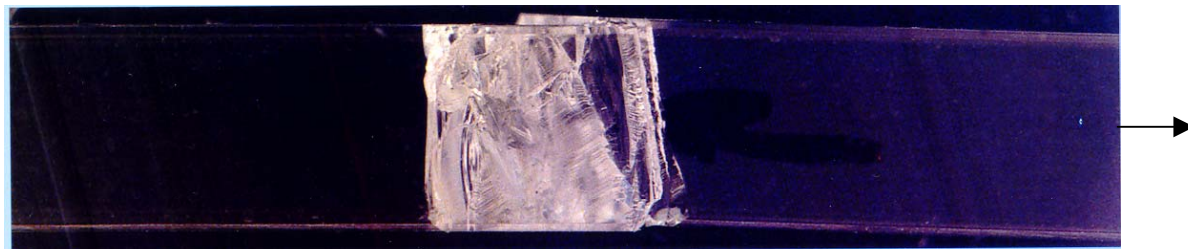
Figure 13 shows that Grafoil has this strong effect in 4-point flexure tests *only* when the c-axis is the principal axis of the specimen (Type 3 and 3a orientations). In Type 1 and 4a orientations, in which the principal stress is along the a-axis, there is no significant difference between the strengths of samples tested with or without Grafoil.

A graph of load vs. displacement during a mechanical test can provide information on events that occur during the test. Most ceramic materials yield a nearly straight line of increasing load with increasing displacement during the mechanical test, as in the upper part of Figure 14 for sapphire tested without Grafoil.<sup>18</sup> When tested with Grafoil, a sawtooth pattern was observed for all three





Twins observed when Grafoil was not used (strength = 234 MPa)



No twins observed when Grafoil was used (strength = 817 MPa)

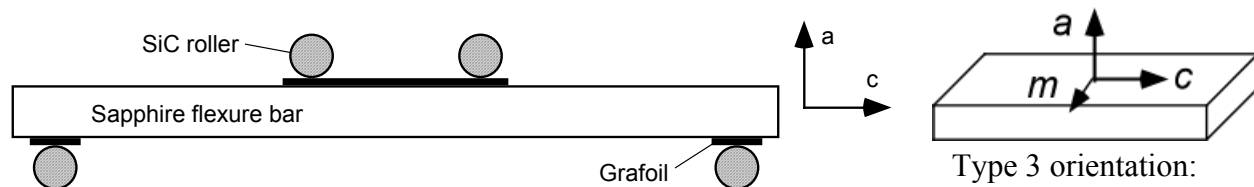


Figure 12. Type 3 flexure specimens tested with or without Grafoil at 600°C using a test fixture with a 10 mm load span and 40 mm support span.<sup>16,17</sup> Czochralski-grown sapphire from Crystar was polished to a 60/40 scratch/dig specification at Meller Optics and then annealed at 1200°C for 24 h in air. Photos were taken with crossed polarizers. The mean strength of 18 bars tested without Grafoil was  $230 \pm 28$  MPa and all were twinned. The mean strength of 9 bars tested with Grafoil was  $547 \pm 156$  MPa and only 2 had macroscopic twinning.

orientations in the lower part of Figure 14. Even Type 4a, which has no compression along the c-axis and does not produce twins, exhibits a sawtooth curve. From these observations, it was hypothesized that the sawtooth behavior was an effect of Grafoil deformation. This hypothesis was supported by the fact that the onset of ratcheting occurred at the same load ( $\sim 350$  N) for all three orientations, while the onset of twinning would be strongly dependent on orientation.

To test the hypothesis, polycrystalline alumina was tested with and without Grafoil at 600°C, but *no sawtooth pattern was observed* in the load-displacement curve. The sawtooth pattern appears to be unique to single-crystal sapphire, possibly due to load adjustment taking place in the compliant Grafoil layer as load is transmitted from unconstrained rollers to the sapphire in a discontinuous motion. In the flexure test, Grafoil acts not only to distribute the load and reduce contact stress, but also to change the friction coefficient between load rollers and the specimen.

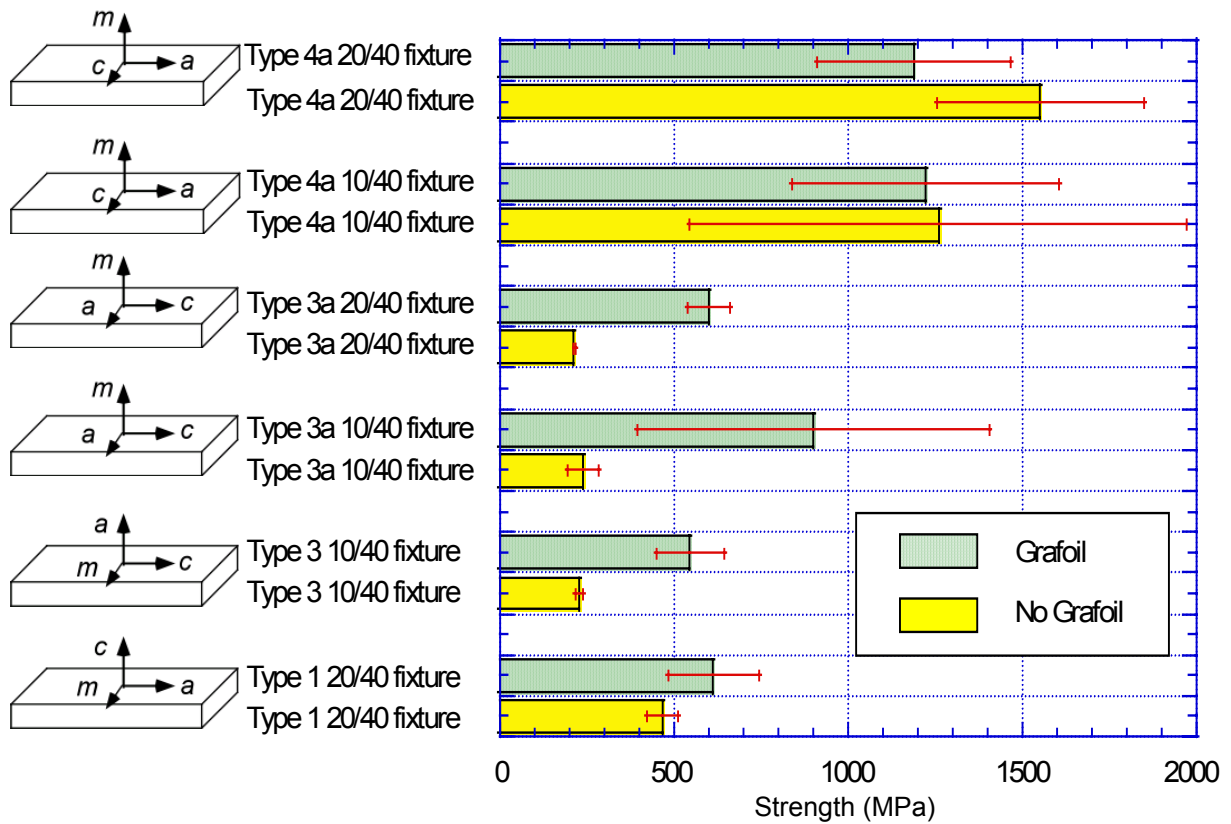


Figure 13. 4-Point flexure strength of sapphire tested with or without Grafoil at 600°C.<sup>18</sup> Fixture dimensions (e.g., 10/40) are the inner and outer load spans in mm. Error bars are 90% confidence intervals for the mean.

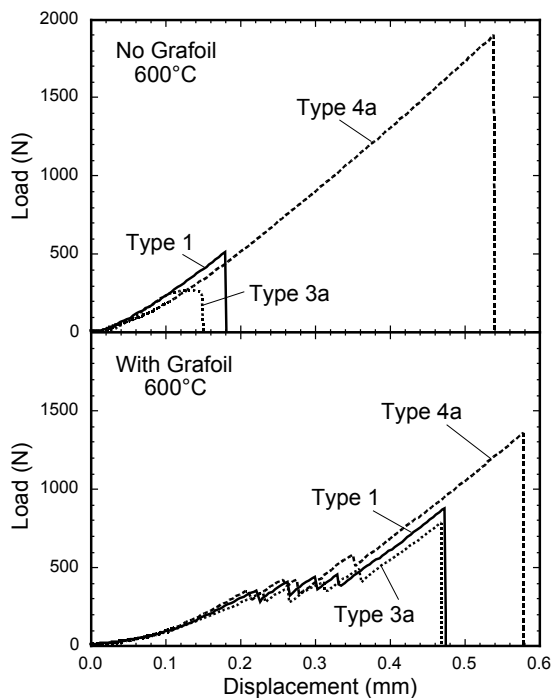


Figure 14. Load-displacement curves for 4-point flexure of sapphire at 600°C without or with Grafoil.<sup>18</sup> Flexure testing of polycrystalline alumina gave curves similar to the upper traces, without the sawtooth behavior seen in the lower traces.

## SLOW CRACK GROWTH IN SAPPHIRE

There is interest in the temperature dependence of the crack growth rate in sapphire for the purpose of predicting propagation of cracks at high temperature in domes and windows. Crack growth rates were measured at the National Institute of Standards and Technology by two methods shown in Figure 15.<sup>19</sup> In dynamic fatigue, the stress required to break a specimen is measured as a function of the stress rate. If cracks propagate during the test, then the slower the stress rate, the more the cracks propagate, and the less stress is required to break the specimen.

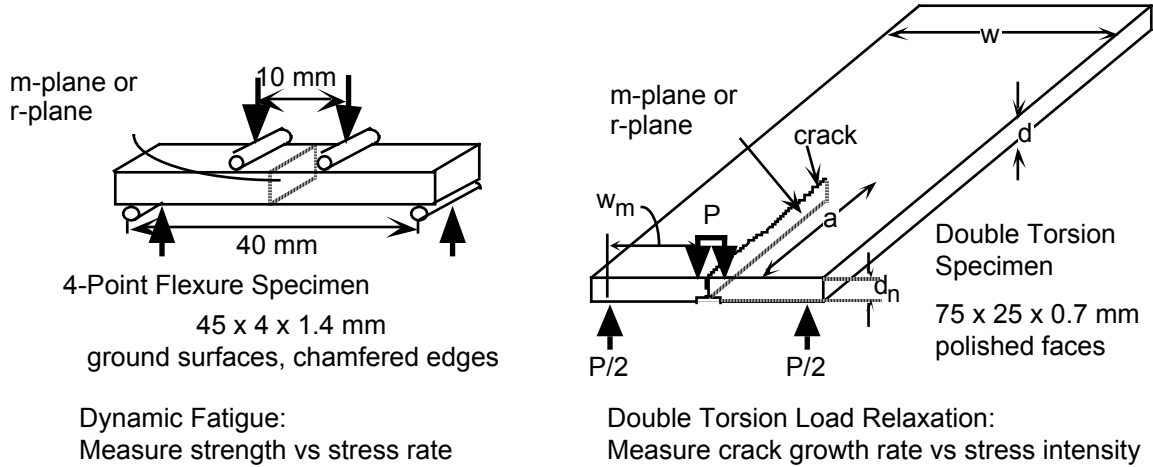


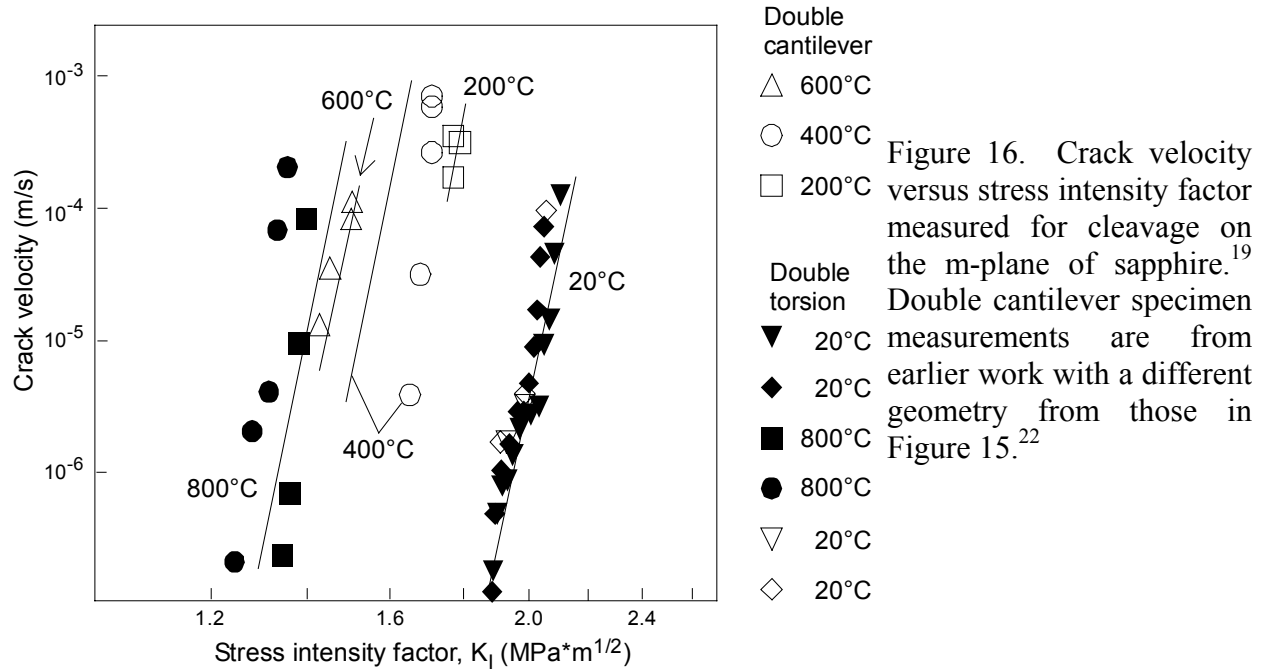
Figure 15. Specimens for measuring the rate of slow crack growth.<sup>19</sup> Crystal orientations were chosen for crack propagation on the m- or r-planes.

In double torsion load relaxation in Figure 15, load  $P$  is applied to a precracked plate whose geometry is such that the stress intensity factor,  $K_I$ , is independent of the length of the crack. (The stress near a crack tip is proportional to the stress intensity factor.) The specimen is quickly loaded until crack propagation begins. Then the displacement of the test fixture is halted and the rate of change of load is measured as the crack propagates and the load relaxes. The crack velocity and stress intensity factor can be computed from measurements of load vs. time during the relaxation.

Figure 16 shows results for m-axis crack propagation from double torsion experiments and earlier work with a different geometry.<sup>22</sup> Data points for 20°, 200°, 400°, 600°, and 800°C were fit to the equation

$$a_1 \ln(v) = \ln(K_I) - a_0 - \frac{a_2}{RT} \quad (1)$$

where  $v$  is the crack velocity (m/s),  $K_I$  is the stress intensity factor ( $\text{MPa}\sqrt{\text{m}}$ ),  $R$  is the gas constant (8.3145 J/K),  $T$  is temperature (K), and the values of the parameters are  $a_0 = 0.4141 \pm 0.02665$ ,  $a_1 = 0.01940 \pm 0.00237$ , and  $a_2 = 1272.3 \pm 42.6$ . Equation (1) is a logarithmic rearrangement of a more familiar equation of the form



$$v = v_0 \left( \frac{K_I}{K_0} \right)^n e^{-E_a/RT} \quad (2)$$

where  $v_0$  is a constant,  $K_0 = 1 \text{ MPa}\sqrt{\text{m}}$  to cancel the units of  $K_I$ ,  $n$  is a dimensionless exponent, and  $E_a$  is the activation energy (J). The relation between the parameters of Equations (1) and (2) are  $n = 1/a_1$ ,  $E_a = a_2/a_1$ , and  $\ln(v_0) = -a_0/a_1$ .

The straight lines in Figure 16 show that Equation (1) fits the data at 20°, 200°, 600°, and 800°C, but not at 400°C. Equation (1) was used to generate the curves in Figure 17, which show that the

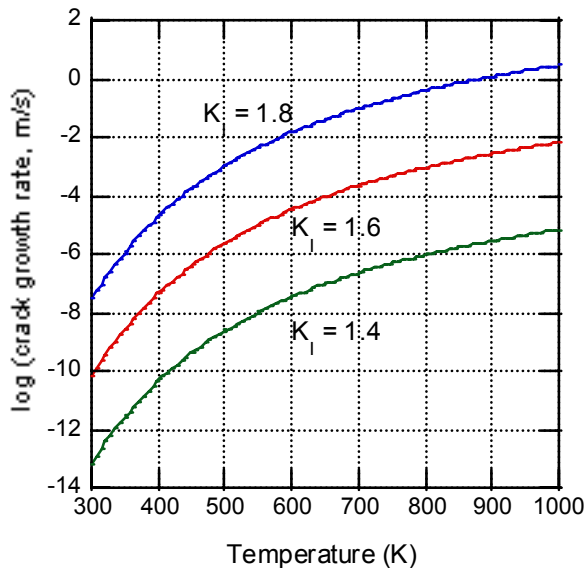


Figure 17. Crack velocity versus temperature calculated from Equation (1).

crack growth rate increases by 7 orders of magnitude between 300 and 1000 K for each stress intensity factor. Clearly, a crack that grows at an insignificant rate at low temperature can grow at a catastrophic rate at the temperature of a hot dome or window.

Measurements of crack growth rate on the r-plane as a function of temperature gave significantly different results on two different specimens. Therefore, no attempt was made to derive an equation for crack growth rate versus temperature for the r-plane.

For m-plane dynamic fatigue specimens in Figure 15, fracture occurred on the m-plane at 20°C, but on the r-plane at 800°C.<sup>19</sup> For r-plane dynamic fatigue specimens, cracks propagated ~9° off the r-plane at both 20° and 800°C. Double torsion specimens behaved in an even more complicated manner. Specimens designed to fracture on the m-plane exhibited a conchoidal fracture surface with no evidence for a preferred cleavage plane.

The double torsion specimens designed to fracture on the r-plane had the most complicated behavior. Panel a of Figure 18 is a macro view of a crack propagating from left to right. In the first brightly shining segment at the left, the fracture surface is at an angle of 5-10° off the r-plane. Then the crack suddenly jumped onto the r-plane at point b and moved ~4 mm before switching off the r-plane again at c and then onto the r-plane once again at the right side of the photo. Panel b shows the fracture surfaces at the transition near point b and panel c shows the fracture surfaces near point c. Crack propagation on the r-plane gives a smooth fracture surface. Crack propagation off the r-plane gives a rough surface. Crack propagation in Figure 18 on the r-plane was much more rapid than propagation off the r-plane. Yet, the crack jumped on and off the r-plane as it propagated from left to right.

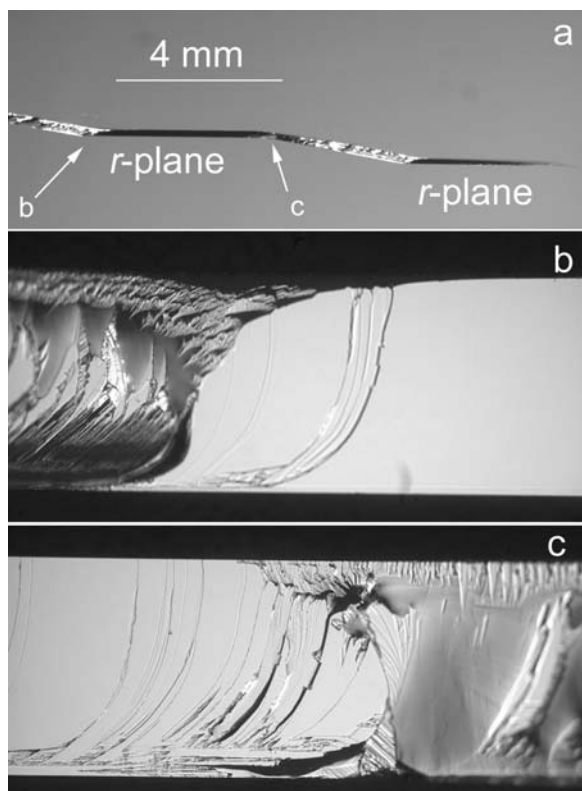


Figure 18. Crack propagation in r-plane double torsion specimen at 20°C.<sup>19</sup>

Figure 19 compares slow crack growth rates at room temperature reported by the National Institute of Standards and Technology<sup>19,22</sup> with those reported by the National Aeronautics and Space Administration.<sup>23</sup> NIST samples were tested in a dry nitrogen atmosphere, whereas NASA samples were immersed in distilled water. The NIST data sets for the r-plane from 2002 come from the samples that gave the erratic crack growth shown in Figure 18. The two replicate specimens did not agree very well with each other. The NIST r-plane data from 1973 in Figure 19 were obtained from a crack that did propagate on the r-plane without switching to another plane. Propagation on the r-plane occurs at approximately half the stress intensity required for propagation that jumps on and off the r-plane.

The NASA crack velocity lines in Figure 19 were calculated from the equations reported in Reference 23. The NIST m-plane line in Figure 19 was calculated from Equation (1) with  $T = 293$  K. The NASA a-plane crack velocity is similar to the NIST m-plane crack velocity, in accord with the notion that the a- and m-planes are physically similar to each other. However, NASA tests are for exposing surfaces in water and NIST surfaces were exposed to dry nitrogen. We would expect that opening a surface under water would be a lower energy process than opening in under chemically inert conditions. It is also of interest that the NASA r-plane data is somewhat similar to the NIST r-plane data from 2002, and that both differ substantially from the NIST data from 1973 in which fracture was believed to occur on the r-plane.

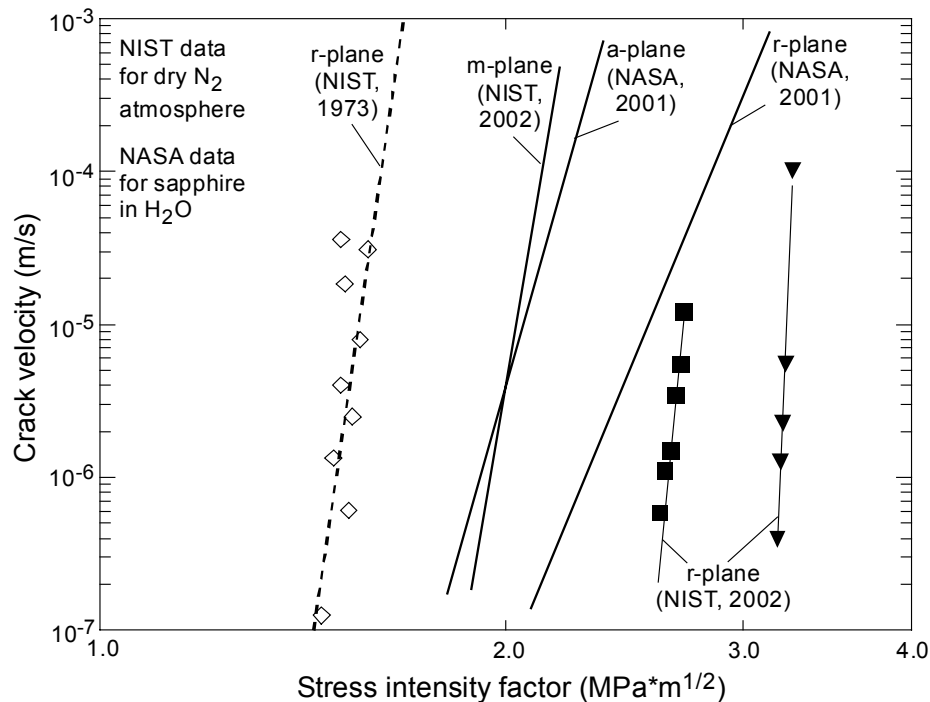


Figure 19. Comparison of slow crack growth rates on different planes of sapphire at 20°C as reported by NIST<sup>19,22</sup> and NASA.<sup>23</sup>

## ACKNOWLEDGEMENTS

Many of the flexure strength results described in this paper were obtained by Crystal Systems under the leadership of Fred Schmid and Chandra Khattak. Slow crack growth studies were conceived and carried out at the National Institute of Standards and Technology by Sheldon Wiederhorn and Ralph Krause, Jr. Most of the work described in this paper was supported by the Office of Naval Research.

## REFERENCES

- <sup>1</sup> J. B. Wachtman, Jr. and L. H. Maxwell, "Strength of Synthetic Single Crystal Sapphire and Ruby as a Function of Temperature and Orientation," *J. Am. Ceram. Soc.*, **1959**, 42, 432.
- <sup>2</sup> E. A. Jackman and J. P. Roberts, "Strength of Synthetic Single-Crystal and Polycrystalline Corundum," *Phil. Mag.*, **1955**, 46, 809; E. A. Jackman and J. P. Roberts, "Strength of Polycrystalline and Single-Crystal Corundum," *Trans. Brit. Ceram. Soc.*, **1955**, 54, 389.
- <sup>3</sup> R. L. Gentilman, E. A. Maguire, H. S. Starrett, T. M. Hartnett and H. P. Kirchner, "Strength and Transmittance of Sapphire and Strengthened Sapphire," *J. Am. Ceram. Soc.*, **1981**, 64, C11.
- <sup>4</sup> R. J. Charles and R. R. Shaw, "Delayed Failure of Polycrystalline and Single-Crystal Alumina," General Electric Research Laboratory Report 62-RL-3081M (1962).
- <sup>5</sup> D. C. Harris, "Overview of Sapphire Mechanical Properties and Strategies for Strengthening Sapphire," *Proc. 7th DoD Electromagnetic Windows Symposium*, Applied Physics Laboratory, Laurel MD, May 1998.
- <sup>6</sup> C. P. Khattak, K. Schmid, F. Schmid, and D. C. Harris, "High Temperature Strength of Doped and Undoped Sapphire," *Proc. 7th DoD Electromagnetic Windows Symposium*, Applied Physics Laboratory, Laurel MD, May 1998.
- <sup>7</sup> D. C. Harris, "Overview of Progress in Strengthening Sapphire at Elevated Temperature," *Proc. SPIE*, **1999**, 3705, 2.
- <sup>8</sup> F. Schmid, K. Schmid, C. P. Khattak, P. R. Duggan and D. C. Harris, "Increasing the Strength of Sapphire by Heat Treatments," *Proc. SPIE*, **1999**, 3705, 36.
- <sup>9</sup> F. Schmid, C. P. Khattak, K. A. Schmid and D. C. Harris, "Increase of High Temperature Strength of Sapphire by Polishing, Heat Treatments, and Doping," *Proc. SPIE*, **2000**, 4102, 43.
- <sup>10</sup> F. Schmid, C. P. Khattak, S. G. Ivanova, D. M. Felt, and D. C. Harris, "Influence of Polishing on the Biaxial Flexure Strength of Sapphire at 600°C," *Proc. 8th DoD Electromagnetic Windows Symposium*, Boulder, Colorado, April 2000.
- <sup>11</sup> E. Savrun, W. D. Scott and D. C. Harris, "Effect of Titanium Doping on the High-Temperature Rhombohedral Twinning of Sapphire," *J. Mater. Sci.*, **2001**, 36, 2295.
- <sup>12</sup> A. Kirkpatrick, D. C. Harris and L. F. Johnson, "Effect of Ion Implantation on the Strength of Sapphire at 300-600°C," *J. Mater. Sci.*, **2001**, 36, 2195.
- <sup>13</sup> T. M. Regan, D. C. Harris, R. M. Stroud and J. R. White, "Neutron Irradiation for Sapphire Compressive Strengthening. I. Processing Conditions and Compressive Strength," *J. Nucl. Mater.*, **2002**, 300, 39.

- <sup>14</sup> T. M. Regan, D. C. Harris, D. W. Blodgett, K. C. Baldwin, J. A. Miragliotta, M. E. Thomas, M. J. Linevsky, J. W. Giles, T. A. Kennedy, M. Fatemi, D. R. Black, and K. P. D. Lagerlöf, "Neutron Irradiation for Sapphire Compressive Strengthening. II. Physical Property Changes," *J. Nucl. Mater.*, **2002**, 300, 47.
- <sup>15</sup> F. Schmid and D. C. Harris, "Effect of Crystal Orientation and Temperature on the Strength of Sapphire," *J. Am. Ceram. Soc.*, **1998**, 81, 885.
- <sup>16</sup> R. Cayse, P. Lagerlöf, R. Polvani, D. Harris, D. Platus, D. McClure, C. Patty and D. Black, *Sapphire Statistical Strength Characterization and Risk Reduction (SSCARR) Program Final Report*, Nichols Research Corp., Huntsville AL, SETAC Contract DASG60-97-D-002, 28 April 2000.
- <sup>17</sup> D. R. McClure, R. W. Cayse, S. Goodrich, D. McCullum, D. C. Harris, K. P. D. Lagerlöf, C. E. Patty, Jr., D. H. Platus, R. S. Polvani, and David R. Black, "Sapphire Statistical Strength Characterization and Risk Reduction Program," *Proc. SPIE.*, **2001**, 4375, 20.
- <sup>18</sup> S. G. Ivanova, F. Schmid, C. P. Khattak and D. C. Harris, Use of Grafoil in Mechanical Testing of Sapphire at Elevated Temperature," *Proc. SPIE.*, **2000**, 4102, 37.
- <sup>19</sup> S. M. Wiederhorn and R. F. Krause, Jr., "Crack Growth in Sapphire," *Ceram. Eng. Sci. Proc.* **2002**, 23, in press.
- <sup>20</sup> W. D. Scott and K. K. Orr, "Rhombohedral Twinning in Alumina," *J. Am. Ceram. Soc.* **1983**, 66, 27.
- <sup>21</sup> G. F. Hurley, "Mechanical Behavior of Melt-Grown Sapphire at Elevated Temperature," *Appl. Polymer Symp. No. 21*, John Wiley & Sons, New York, 1973, pp. 121-130.
- <sup>22</sup> S. M. Wiederhorn, B. J. Hockey, and D. E. Roberts, "Effect of Temperature on the Fracture of Sapphire," *Phil. Mag.* **1973**, 28, 783.
- <sup>23</sup> J. L. Salem, L. Powers, R. Allen, and A. Calomino, "Slow Crack Growth and Fracture Toughness of Sapphire for a Window Application," *Proc. SPIE* **2001**, 4375, 41; J. L. Salem, A. Calomino, R. Allen, and L. Powers, "Slow Crack Growth of Sapphire," *Ceram. Eng. Sci. Proc.* **2002**, 23, in press.